SPANDIDOS PUBLICATIONS

INTERNATIONAL JOURNAL OF MOLECULAR MEDICINE 49: 56, 2022

Hydrogen sulfide attenuates cigarette smoke-induced pyroptosis through the TLR4/NF-κB signaling pathway

LIANG WANG[1*], JING MENG[1*], CAICAI WANG[1*], YUAN WANG[1], CHAO YANG[2] and YUJING LI[3]

[1]Department of Respiratory and Critical Care, Hebei Chest Hospital; [2]Department of Gynecology, Shijiazhuang Second Hospital; [3]Laboratory of Medicine, Hebei Chest Hospital, Shijiazhuang, Hebei 050048, P.R. China

Received December 10, 2021; Accepted February 11, 2022

DOI: 10.3892/ijmm.2022.5112

Abstract. Pyroptosis, a type of programmed cell death mediated by caspases-1 or -11, may play an important role in airway epithelial injury and airway remodeling, thereby promoting the occurrence of asthma and chronic obstructive pulmonary disease (COPD). Studies have suggested that hydrogen sulfide (H_2S) plays a protective role against COPD by inhibiting the activation of the NLR family pyrin domain containing 3 (NLRP3) inflammasome. The present study established a rat model of cigarette smoke (CS)-induced COPD to observe the effects of H_2S on cell pyroptosis. A 16HBE cell model was also used to further examine the effects of H_2S on the Toll-like receptor 4 (TLR4)/NF-κB signaling pathway is affected by, and to determine the underlying mechanisms. The results revealed that cell pyroptosis was significantly promoted in the model of CS-induced COPD. The cellular experiments also revealed that CS induced the pyroptosis of the cells in a NLRP3/gasdermin D (GSDMD)-dependent manner. In addition, H_2S significantly attenuated the effects of CS extract (CSE) on pyroptosis, cell viability and the expression levels of pyroptosis-related proteins, indicating that H_2S inhibited pyroptosis by decreasing NLRP3 expression and promoting GSDMD activation. It was also identified that CSE activated TLR4 protein in 16HBE cells, while this was inhibited by H_2S. Furthermore, TLR4 and NF-κB overexpression significantly abolished the effects of H_2S on cell pyroptosis. On the whole, the findings of the present study demonstrate the role of pyroptosis in the development of COPD and provide an experimental basis for the use of H_2S and drugs targeting the TLR4/NF-κB pathway to exert protective effects against COPD.

Correspondence to: Dr Chao Yang, Department of Gynecology, Shijiazhuang Second Hospital, 53 Huaxi Road, Xinhua, Shijiazhuang, Hebei 050048, P.R. China
E-mail: yangchao124517@126.com

Dr Yujing Li, Laboratory of Medicine, Hebei Chest Hospital, 372 Shengli North Street, Chang'an, Shijiazhuang, Hebei 050048, P.R. China
E-mail: liyujing1982@sina.com

[*]Contributed equally

Key words: hydrogen sulfide, chronic obstructive pulmonary disease, cigarette smoke, Toll-like receptors 4, NF-κB

Introduction

Chronic obstructive pulmonary disease (COPD) is a chronic airway inflammatory disorder; it is a common respiratory illness and the third highest cause of mortality in China (1). COPD has attracted increased worldwide attention due to its high incidence, morbidity and mortality rates (2). It is characterized by an irreversible expiratory airflow limitation and manifests as a chronic inflammatory disorder and pulmonary emphysema (3). The primary risk factor for COPD is exposure to cigarette smoke (CS). Research using animals has revealed that frequent exposure to CS can enhance the number of inflammatory factors, such as tumor necrosis factor (TNF), in the alveolar space and lung parenchyma (4). A recent study reported that the incidence rate of COPD among Chinese adults aged >40 years was 13.7%, and revealed that smoking and particulate matter 2.5 were the main causes of COPD (5). According to statistics, >70% of patients with COPD have a history of smoking (6). The early prevention and treatment of COPD remain a challenge worldwide. Therefore, studying its pathogenesis is crucial for proposing novel therapeutic strategies for the early prevention and treatment of COPD.

Cell pyroptosis is a type of programmed cell death mediated by Caspase-11 or -1. Under physiological conditions, pyroptosis is crucial for organ development (7). When cell pyroptosis occurs, the cell membrane rapidly ruptures and forms a pore-like membrane structure, through which several inflammatory agents and the cell content are released (8). When exogenous microorganisms and stress result in the production of Caspase-1, which is triggered and activated by the inflammasome, gasdermin D (GSDMD) is cleaved to form the N-terminal fragment of GSDMD (GSDMD-N), which further induces the formation of the membrane pore and the release of inflammatory factors. Recent studies have revealed that pyroptosis is a common occurrence in respiratory illnesses; therefore, inhibiting the occurrence of pyroptosis in the respiratory system may minimize the degree of lung cell injury, as well as the production of the inflammatory response and its associated factors (9-13). Tsai *et al* (14) reported that the NLR family

pyrin domain containing 3 (NLRP3) inflammasome promoted the apoptosis of bronchial epithelial cells and induced airway epithelial injury and airway remodeling, thereby promoting the occurrence of asthma and COPD. It has been reported that CS extract (CSE) induces the pyroptosis of human bronchial epithelial cells by activating NLRP3/Caspase-1 signaling, thereby aggravating COPD development (15). Similarly, adipose stem cell-derived exosomes can mitigate CS-induced pyroptosis, and thus inhibit COPD development (16). Therefore, reducing pyroptosis may serve as an effective approach for preventing the progression of COPD.

Hydrogen sulfide (H_2S) is a toxic gas with an odor of rotten egg (17). H_2S is now considered as the third gas signal molecule after carbon monoxide and nitric oxide (18). Furthermore, it participates in a variety of signal transduction pathways and plays a protective role through its antioxidant, anti-apoptotic and anti-inflammatory effects in various pathological cells, as well as organs. Studies have demonstrated that H_2S can protect cells from damage in different disease models by activating different signaling pathways. For example, H_2S has been shown to attenuate lipopolysaccharide (LPS)-induced acute lung injury in mice through the activation of the PI3K/Akt/mTOR pathway (19). Similarly, H_2S has been found to inhibit thyroxin-induced myocardial fibrosis in rats by activating the PI3K/Akt signaling pathway (20). It has also been demonstrated that H_2S alleviates age-related macular degeneration by inhibiting inflammation and oxidative stress-mediated pyroptosis (21). Furthermore, a previous study by the authors revealed that H_2S attenuated CS-induced COPD by inhibiting the transforming growth factor-β1/Smad pathway, suggesting that H_2S may serve as a potential therapeutic agent for COPD (22). However, whether the beneficial effects of H_2S are dependent on its impact on cell pyroptosis remains unknown. Therefore, the aim of the present study was to establish a rat model of CS-induced COPD to observe the effects of H_2S on cell pyroptosis. A 16HBE cell model was also established to further examine the effects of H_2S on the Toll-like receptor (TLR)4/NF-κB signaling pathway may be affected by and to elucidate the underlying mechanisms.

Materials and methods

Animals. A total of 48 male Sprague-Dawley rats, weighing 250-270 g (9-10 weeks old), were purchased from the Hebei Chest Hospital Animal Center. The animal procedures were approved by the Animal Ethics Committee of the Hebei Chest Hospital Animal Center and complied with the Guide of the Care and Use of Laboratory Animals published by the National Institutes of Health (23). All rats were provided with water and food *ad libitum* and were examined at the pathogen-free barrier laboratory of the Hebei Chest Hospital Animal Center (Shijiazhuang, China). The rats where maintained in a laboratory with a 12-h light/dark cycle, a temperature of <23˚C and a humidity of 35%. Every attempt was made to reduce animal distress and pain. The rats were housed in a holding house for adaptation for 5 days following their arrival at the laboratory.

Model of CS-induced COPD. The rats were randomly assigned into different groups (n=12 per group) as follows: The H_2S, CS + H_2S, CS and control groups. The rat model of COPD was established according to the study by Ke *et al* (24). CS inhalation by rats in the CS + H_2S and CS groups was performed using the Buxco inhalation exposure system (Data Sciences International, Inc.) for 28 weeks. Derby cigarettes (Wuhu Cigarettes Factory) were used to generate the smoke. Each cigarette contained 0.9 mg nicotine, 10 mg tar and 12 mg carbon monoxide. The rats were treated with a 20-cigarette equivalent inhalation for 2 h and then permitted to rest for 4 h on the same day. The rats breathed the CS for 6 days a week. The rats in the sham (control group) inhaled air for 28 weeks using the Buxco animal CS-exposure system, and then inhaled air inside a plastic 20-liter container for 7 days.

H_2S inhalation. During H_2S inhalation, the rats were placed in a plastic 20-liter container and permitted to inhale air combined with H_2S for 8 h every day for 7 days following the establishment of the model of CS-induced COPD. H_2S flowed through a flowmeter and regulator, and blended into the air. The flow of air, including H_2S, was regulated to maintain the H_2S concentration at 40 ppm. Non-COPD model rats also breathed 40 ppm H_2S for 8 h every day for 7 days. H_2S was purchased from the Shijiazhuang Zhongyuan Specialty Gas Co., Ltd. The concentration of H_2S was measured using a H_2S concentration monitor (HG-BX-H_2S, Haigu Co.; https://www.czhaigu.com/aboutus.html).

Histopathological analysis. The rats were anesthetized with pancuronium bromide [0.6 mg/kg, intraperitoneal (i.p.)] and sodium pentobarbital (100 mg/kg, i.p.) following the inhalation of H_2S. Cervical dislocation was used as the method of sacrifice and a thoracotomy was performed to expose the lungs. The lungs were perfused via the right ventricle with 30 ml ice-cold sterile phosphate-buffered saline (PBS). The left lung lobes were extracted and preserved at 25˚C with 4% formalin for 48 h. The lung was then sliced into 4-μm-thick sections for further histological analysis.

For hematoxylin and eosin (H&E) staining, the protocol used was as previously described (25). Briefly, the sections were blocked with 3% hydrogen peroxide for 20 min, and non-specific binding sites were blocked with QuickBlock™ immunostaining blocking reagent (Beyotime Institute of Biotechnology) for 1 h. The sections were then incubated with (H&E; Beyotime Institute of Biotechnology) sequentially at room temperature for 20 min and washed. All images were captured on an optical microscope (Carl Zeiss AG).

Immunohistochemistry (IHC). Paraffin-embedded sections, as well as block fabrication, were conducted in the same manner as described above for H&E staining (26). IHC staining for GSDMD-N was performed on the lung tissue slides from each group. The lung tissue slides were heated for 20 min in a microwave (100˚C) with 0.01 M citrate buffer (pH 6.0), and were cooled down gently to room temperature. Following retrieval, the slides were incubated for ~30 min at room temperature with 3% H_2O_2 (Sigma-Aldrich, Merck KGaA). They were then blocked with 5% BSA (Beyotime Institute of Biotechnology) supplemented with 10% normal goat serum (Beyotime Institute of Biotechnology) and PBS plus Tween-20 (Beyotime Institute of Biotechnology) at room temperature for 1 h to inhibit non-specified protein binding.

This was followed by incubation with an anti-GSDMD-N rat monoclonal primary antibody (dilution, 1:200; PA5-104324, Invitrogen; Thermo Fisher Scientific, Inc.) at 4˚C overnight. An IgG secondary antibody (dilution, 1:500; BA-4000; Vector Laboratories, Inc.) was used in the biopsy to examine the expression of the primary antibody, and was incubated with the sections for 30 min at 37˚C. Avidin-biotin complex reagent (ABC kit; Vector Laboratories, Inc.) was used to treat the slides for 30 min at room temperature. The sections were then incubated with 3,3'-diaminobenzidine (Sigma-Aldrich, Merck KGaA) tetrahydrochloride hydrate solution for 2 min at room temperature. Using the Slide view VS200 Scanner (Olympus Corporation), GSDMD-N expression was detected and captured digitally.

Western blot analysis. First, RIPA buffer (Sigma-Aldrich, Merck KGaA) was used to extract protein from the cultured cells or rat tissues. The protein lysate was then separated using 15% sodium dodecyl sulphate-polyacrylamide gel electrophoresis and transferred onto a difluoride polyvinylidene membrane. The amount and quality of the protein was examined using BCA assay (Beyotime Institute of Biotechnology) in a Synergy H1 microplate reader (BioTek Instruments, Inc.). Equal amounts of protein per lane (mass of 20 μl) were then loaded onto a 12% gel from a TGX Stain-Free FastCast Acrylamide kit (Bio-Rad Laboratories, Inc.) and finally transferred onto a 0.45 μm PVDF membrane (GE Healthcare, Inc.). The membrane was blocked with 5% non-fat milk-PBS for 1 h at room temperature and was then incubated overnight at 4˚C with the following antibodies: NLRP3 (dilution, 1:1,000; cat. no. sc-134306; Santa Cruz Biotechnology, Inc.), cleaved Caspase-1 (dilution, 1:1,500; cat. no. YC0002; ImmunoWay Biotechnology Company), Caspase-1 (dilution, 1:800; cat. no. PA5-99477; Invitrogen; Thermo Fisher Scientific, Inc.), cleaved IL-1β (dilution, 1:1,000; cat. no. 83186; Cell Signaling Technology, Inc.), IL-1β (dilution, 1:1,000; cat. no. P420B; Thermo Fisher Scientific, Inc.), cleaved GSDMD (dilution, 1:1,000; cat. no. ab215203; Abcam, Inc.), pro-GSDMD (dilution, 1:1,000; cat. no. sc-81868; Santa Cruz Biotechnology, Inc.), TLR4 (dilution, 1:1,000; cat. no. sc-293072; Santa Cruz Biotechnology, Inc.), inhibitor κB-α (IκBα, dilution, 1:1,000; cat. no. sc-1643; Santa Cruz Biotechnology, Inc.), phosphorylated (p)-IκBα (dilution, 1:1,000; cat. no. sc-8404; Santa Cruz Biotechnology, Inc.), NF-κB p-p65 (dilution, 1:1,000; cat. no. sc-166748; Santa Cruz Biotechnology, Inc.), NF-κB p50 (dilution, 1:1,000; cat. no. sc-8414; Santa Cruz Biotechnology, Inc.), GAPDH (dilution, 1:1,000; cat. no. 5174; Cell Signaling Technology, Inc.), Histone H3 (dilution, 1:1,000; cat. no. ab1791; Abcam, Inc.) and NF-κB p65 (dilution, 1:1,000; cat. no. sc-8008; Santa Cruz Biotechnology, Inc.). The membranes were washed and incubated with with horseradish peroxidase-conjugated anti-rabbit secondary antibodies (dilution, 1:10,000; cat. no. sc-2357; Santa Cruz Biotechnology, Inc.) or anti-mouse secondary antibody (dilution, 1:10,000; cat. no. sc-2005; Santa Cruz Biotechnology, Inc.) for 2 h at room temperature. Finally, the membranes were washed and antibodies were identified using a SuperSignal West Pico Chemilluminescent Substrate (Thermo Fisher Scientific, Inc.). The band intensity was quantified using ImageJ software (version 1.6.0; National Institutes of Health).

Cells, cell culture and treatment. Immortalized 16HBE cells were acquired from Procell Life Science & Technology Co., Ltd. A total of 10 generations of 16HBE cells were cultured in Dulbecco's modified Eagle's medium (DMEM; Gibco; Thermo Fisher Scientific, Inc.) supplemented with 10% fetal bovine serum (Biological Industries) in room air with 5% CO_2 at 37˚C. The preparation of CSE was performed as previously described (24). The CS was collected into a glass syringe containing 10 ml DMEM. The serum-free DMEM (MilliporeSigma) was then filtered and titrated with sodium hydroxide (NaOH) (Sangon Biotech, Inc.) at pH 7.35-7.45. The liquid was considered to yield the CSE at a concentration of 100%. To achieve suitable concentrations, the liquid was diluted again with DMEM. The CSE was prepared for ~30 min and then used. Subsequently, 5% CSE was used to challenge the 16HBE cells, and the GSDMD inhibitor, necrosulfonamide (NSA; 20 μM; Cell Signaling Technology, Inc.), or the NLRP3 inhibitor, cytokine release inhibitory drug 3 (CRID3; 10 μM; Cell Signaling Technology, Inc.), were added to the culture medium 2 h prior to the CSE challenge. Pyroptosis and cell viability were then measured using lactate dehydrogenase (LDH) release assay and a water soluble tetrazole salt-1 (WST-1) assay, as described below. To examine the effects of H_2S on the CSE-induced pyroptosis of 16HBE cells, the cells were treated with 5% CSE and sodium hydrosulfide (NaHS; an H_2S donor; Thermo Fisher Scientific, Inc.) for 24 h. Pyroptosis, cell viability and the expression of pyroptosis-related proteins were then measured.

Cell viability assay. The 16HBE cells were plated at a density of $2x10^3$ cells/well in a 96-well culture plate and treated with 0.5-10% CSE for 24 h. A WST-1 cell proliferation assay kit (Beyotime Institute of Biotechnology) was used to evaluate 16HBE cell viability. To fully dissolve the WST-1 powder and form its solutions, 5 ml electronic coupling substance was added. Subsequently, 100 μl solution containing 2,000 cells was added to each well. Subsequently, 10 μl WST-1 solution was added to each well followed by incubation for 2 h at room temperature. Finally, a microplate reader (BioTek Instruments, Inc.) was used to measure the optical density at a wavelength of 450 nm.

LDH release assay. The LDH Assay kit (Beyotime Institute of Biotechnology) was used to detect the rate of pyroptosis. Briefly, the culture supernatant of 16HBE cells (120 μl/well) was collected and incubated for 30 min at 25˚C with 60 μl LDH reaction buffer in the dark. The absorbance was measured using a microplate reader (BioTek Instruments, Inc.) at 490 nm.

Induction of TLR4 or NF-κB overexpression via lentiviral vector. Similar to the study of Ding *et al* (27), TLR4, NF-κB and negative control lentiviral vectors were synthesized by GeneChem, Inc. Briefly, 10 μl GV492-TLR4/NC-EGFP, 10 μl GV492-NF-κB/NC-EGFP or 10 μl packing vector were transfected into the 293T cell line (The Cell Bank of Type Culture Collection of the Chinese Academy of Sciences) using Lipofectamine™ 2000 reagent (Invitrogen; Thermo Fisher Scientific, Inc.) for 5 min at room temperature. After 48 h, the viral supernatant was harvested by ultracentrifugation for 1 h at 1,200 x g at 37˚C.

Briefly, the 16HBE cells were cultured into 6-well plates until the cells were ~50% confluent. The cells were then transfected with the 10 μl GV492-TLR4/NC-EGFP, 10 μl GV492-NF-κB/NC-EGFP or 10 μl packing vector (MOI: 50-80). The medium was changed 6 h later, and the cells continued to be cultured for 72 h. The lentivirus-treated 16HBE cells were then treated with 5% CSE and NaHS for 24 h. The transfection efficiency was measured using reverse transcription-quantitative PCR (RT-qPCR).

RT-qPCR. The total RNA was extracted using TRIzol® reagent (Invitrogen; Thermo Fisher Scientific, Inc.) following the manufacturer's protocol. Reverse transcription was then performed using the One-Step SYBR PrimeScript RT-PCR kit (Takara Biotechnology Co., Ltd.). The reaction was performed using the ABI PRISM 7500 Real-Time PCR system (Applied Biosystems; Thermo Fisher Scientific, Inc.) at 42˚C for 5 min, 95˚C for 10 sec, followed by 40 cycles of 95˚C for 5 sec, 55˚C for 30 sec and 72˚C for 30 sec. A total of three independent experiments were conducted each time. The data were then analyzed by comparing the $2^{-\Delta\Delta Cq}$ value (28). The expression of genes was normalized using GAPDH as a loading control. The primers used were as follows: TLR4 upstream, 5'-TGG CATGAAACCCAGAGCTT-3' and downstream, 5'-ACCCGC AAGTCTGTGCAATA-3'; NF-κB upstream, 5'-GGGCAG GAAGAGGAGGTTTC-3' and downstream, 5'-AATAGG CAAGGTCAGGGTGC-3'; GAPDH upstream, 5'-AATGGG CAGCCGTTAGGAAA-3' and downstream, 5'-GCGCCC AATACGACCAAATC-3'.

TLR4 or NF-κB knockdown via lentiviral vector. Similar to the study of Zhang *et al* (29), CRISPR/Cas9-mediated genome editing methods were used in the present study. Briefly, TLR4 or NF-κB single-guide RNAs (sgRNAs) and a scrambled control sequence were cloned into a lentiviral plasmid GV393, separately. The 16HBE cells were then seeded into 6-well plates at a density of $1x10^7$ cells/well and subsequently infected with the lentiviral constructs (MOI: 50-80) following the manufacturer's instructions. The efficacy of TLR4 knockdown was confirmed using western blot analysis. The medium was changed 6 h later, and the cells continued to be cultured for 72 h. The lentivirus-treated 16HBE cells were then treated with 5% CSE and NaHS for 24 h.

Statistical analysis. All data were evaluated using SPSS 17.0. Software (SPSS, Inc.). One-way ANOVA with the Bonferroni post hoc test was performed to examine the quantitative data. Data are presented as the mean ± standard deviation. $P<0.05$ was considered to indicate a statistically significant difference.

Results

H_2S attenuates CS-induced lung injury and pyroptosis. The lung histopathological changes as detected using H&E staining are presented in Fig. 1A. Exposure to CS induced inflammatory cell infiltration and alveolar septum thickening, which were considerably alleviated in the CS + H_2S group. In addition, treatment with H_2S alone did not induce notable histopathological changes. The IHC findings for GSDMD-N expression in the lungs are illustrated in Fig. 1B. In the CS group, the expression of GSDMD-N determined using IHC was markedly increased, while it was markedly decreased by H_2S. Furthermore, GSDMD-N expression was not altered by H_2S alone. Representative results of the western blot analysis of NLRP3, cleaved Caspase-1, Caspase-1, cleaved pro-IL-1β, IL-1β, cleaved GSDMD and pro-GSDMD expression in lung tissue are shown in Fig. 1C and D. Relative changes in the levels of these proteins are presented in Fig. 1E-H. It was found that NLRP3 expression was markedly increased in the CS group, and the ratios of cleaved IL-1β/pro-IL-1β, cleaved Caspase-1/Caspase-1 and cleaved GSDMD/pro-GSDMD were all enhanced, while these were notably decreased by H_2S. The expression levels of these proteins were not affected by H_2S alone. Thus, these results indicated that CS induced lung injury and pyroptosis, which was partly reversed by H_2S.

Effect of CSE on the pyroptosis of 16HBE cells. First, the 16HBE cells were exposed to various concentrations of CSE (0.5-10% of the CSE) for 24 h, and pyroptosis and cell viability were then measured using LDH and WST-1 assay, respectively. The LDH activity was enhanced by CSE in a concentration-dependent manner (Fig. 2A), while cell viability was decreased by CSE in a concentration-dependent manner (Fig. 2B). Subsequently, 5% CSE was selected to treat the 16HBE cells, and the GSDMD inhibitor, NSA, was added to the culture medium. Pyroptosis and cell viability were then measured using LDH and WST-1 assay, respectively. The results demonstrated that pyroptosis was significantly inhibited by NSA (Fig. 2C). Moreover, 5% CSE induced a significant decrease in cell viability, which was partially attenuated by NSA (Fig. 2D). These results revealed that pyroptosis played an essential role in the cytotoxic effects of CSE on 16HBE cells.

CSE increases the expression of pyroptosis-related proteins in 16HBE cells in a concentration-dependent manner. The 16HBE cells were then exposed to various concentrations of CSE (0.5-10%) for 24 h to validate the effects on pyroptosis. The expression of NLRP3, cleaved Caspase-1, cleaved IL-1β, Caspase-1, pro-IL-1β, cleaved GSDMD and pro-GSDMD in the cells was then detected using western blot analysis. Representative results are shown in Fig. 3A and B. The relative changes in the levels of these proteins are shown in Fig. 3C-F. It was demonstrated that NLRP3 expression and the ratios of cleaved IL-1β/pro-IL-1β, cleaved Caspase-1/Caspase-1 and cleaved GSDMD/pro-GSDMD were significantly increased by 1-10% CSE in a concentration-dependent manner.

CSE-induced pyroptosis is inhibited in 16HBE cells by the NLRP3 inhibitor, CRID3. To examine the function of NLRP3 in 16HBE cells undergoing CSE-induced pyroptosis, the cells were exposed to 5% CSE and treated with the NLRP3 inhibitor, CRID3, for 24 h, and pyroptosis and cell viability, as well as the expression levels of pyroptosis-related proteins, were then examined. As shown in Fig. 4A and B, CRID3 significantly reduced the LDH activity and increased the viability of the 16HBE cells. As shown in Fig. 4C-H, CRID3 substantially decreased NLRP3 expression and the ratios of cleaved IL-1β/pro-IL-1β, cleaved Caspase-1/Caspase-1 and

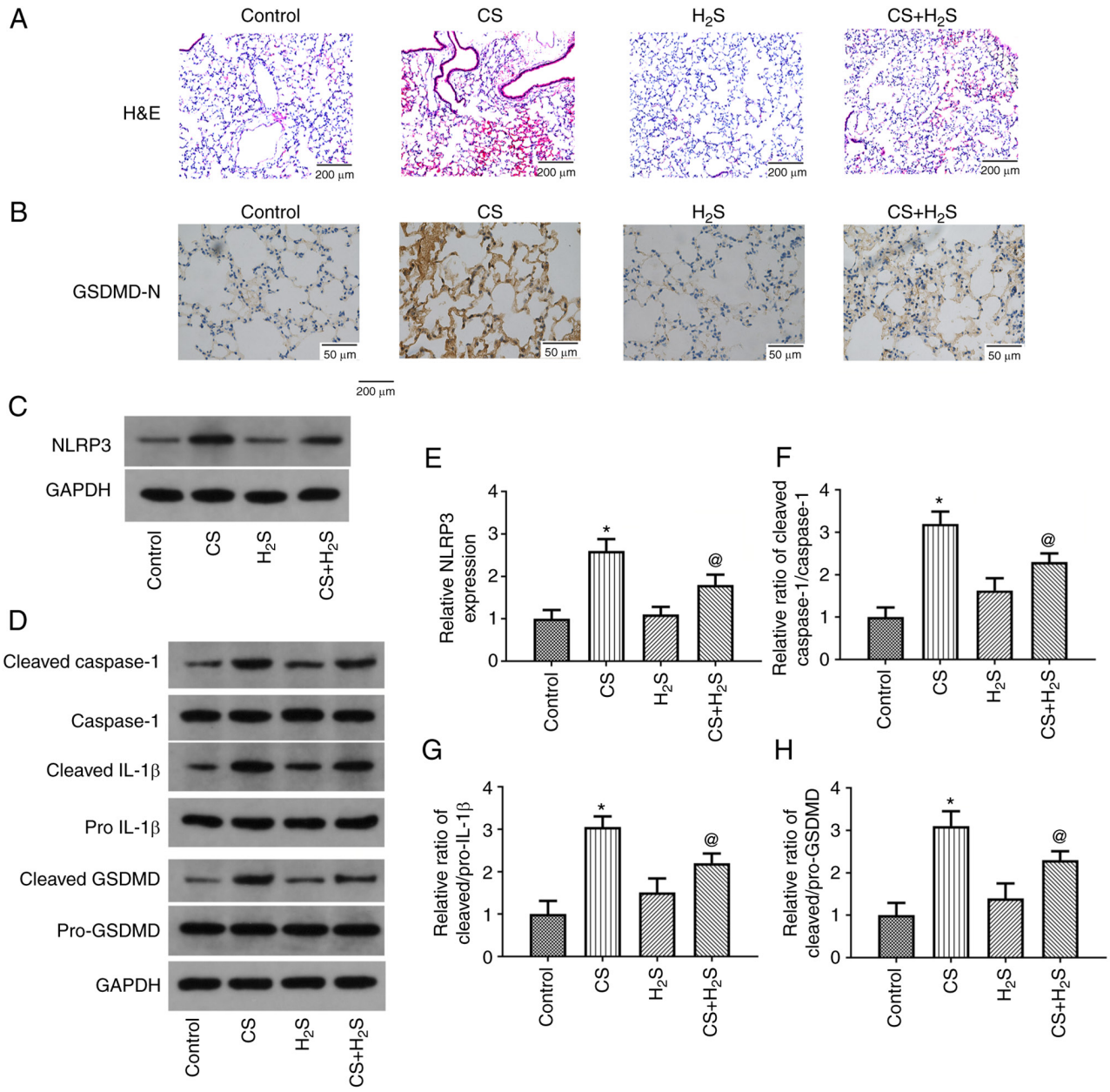

Figure 1. Effect of H_2S inhalation on histopathological appearance of the lung tissue of rats and the expression of pyroptosis-related proteins. (A) H&E staining results. (B) GSDMD-N expression was detected in the lung using immunohistochemistry. (C and D) Representative protein bands of NLRP3, cleaved Caspase-1, Caspase-1, cleaved pro-IL-1β, IL-1β, cleaved GSDMD and pro-GSDMD expression. (E-H) Quantitative results of western blot analysis. Values are presented as the mean ± SD and are representative of three independent experiments. *P<0.05 compared with the control group; @P<0.05 compared with the CS group. H&E, hematoxylin and eosin; GSDMD, gasdermin D; NLRP3, NLR family pyrin domain containing 3; CS, cigarette smoke; H2S, hydrogen sulfide.

cleaved GSDMD/pro-GSDMD. These findings suggested that pyroptosis induced by CSE was dependent on NLRP3 in the 16HBE cells.

NaHS reverses the CSE-induced pyroptosis of 16HBE cells. To examine the effects of H_2S on the CSE-induced pyroptosis of 16HBE cells, the cells were exposed to 5% CSE and treated with NaHS (an H_2S donor) for 24 h. The LDH activity, cell viability and the expression levels of pyroptosis-related proteins were then measured. As shown in Fig. 5A and B, NaHS significantly decreased LDH activity and increased 16HBE cell viability. As shown in Fig. 5D-H, NaHS considerably decreased NLRP3 expression and the ratios of cleaved IL-1β/pro-IL-1β, cleaved Caspase-1/Caspase-1 and cleaved GSDMD/pro-GSDMD. Thus, these findings demonstrated that H_2S decreased the pyroptosis of 16HBE cells induced by CSE.

NaHS suppresses the activation of the TLR4/NF-κB pathway in CSE-challenged 16HBE cells. To examine the role of the TLR4/NF-κB pathway in the effects of H_2S on the CSE-induced pyroptosis of 16HBE cells, the cells were exposed to 5% CSE and NaHS (H_2S donor) for 24 h, and the expression levels of IκBα, p-IκBα, NF-κB p50, NF-κB p65 and NF-κB p-p65 were measured (Fig. 6). The ratios of NF-κB p-p65/p65 and p-IκBα/IκBα, as well as the expression levels of NF-κB p50 and TLR4 in 16HBE cells, were markedly increased by CSE; these effects were partly reversed by NaHS. These findings

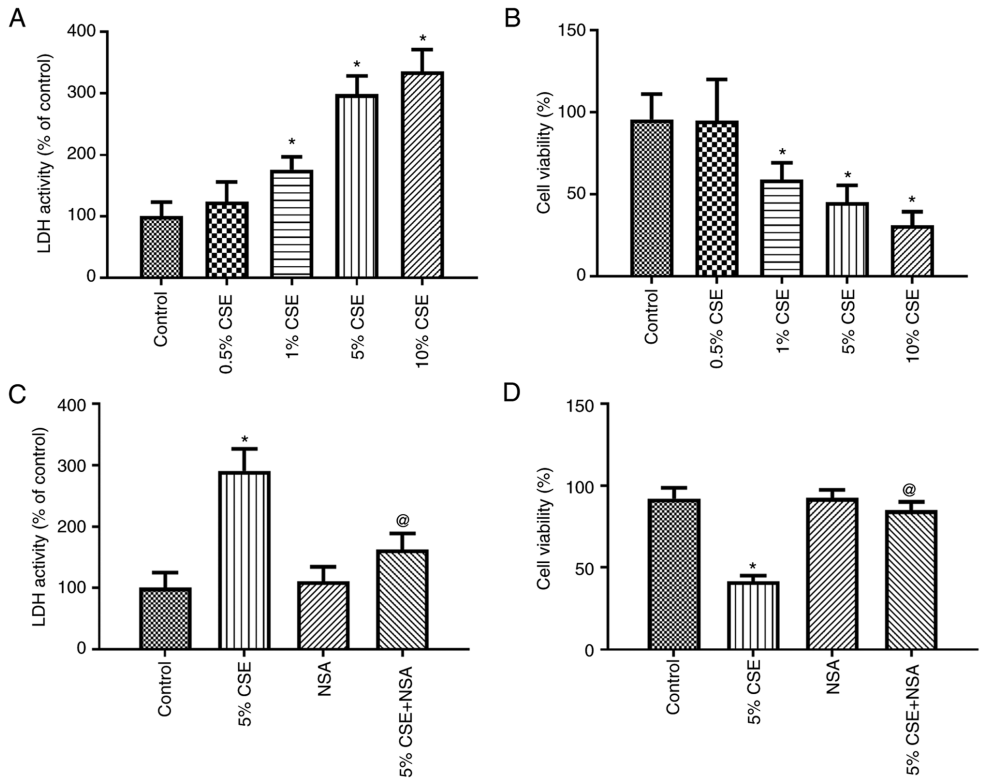

Figure 2. Effects of CSE on the pyroptosis and proliferation of 16HBE cells. The 16HBE cells were exposed to 0.5-10% CSE for 24 h. (A) Pyroptosis was measured using LDH release assay. (B) Cell viability was measured using WST-1 assay. Subsequently, 5% CSE was selected to challenge the 16HBE cells, and the GSDMD inhibitor, NSA, was added to the culture medium. (C) Pyroptosis and (D) cell viability were measured using LDH and WST-1 assay, respectively. Values are presented as the mean ± SD and are representative of three independent experiments. *P<0.05 compared with the control group; @P<0.05 compared with the CSE group. CSE, cigarette smoke extract; GSDMD, gasdermin D; NSA, necrosulfonamide; LDH, lactate dehydrogenase.

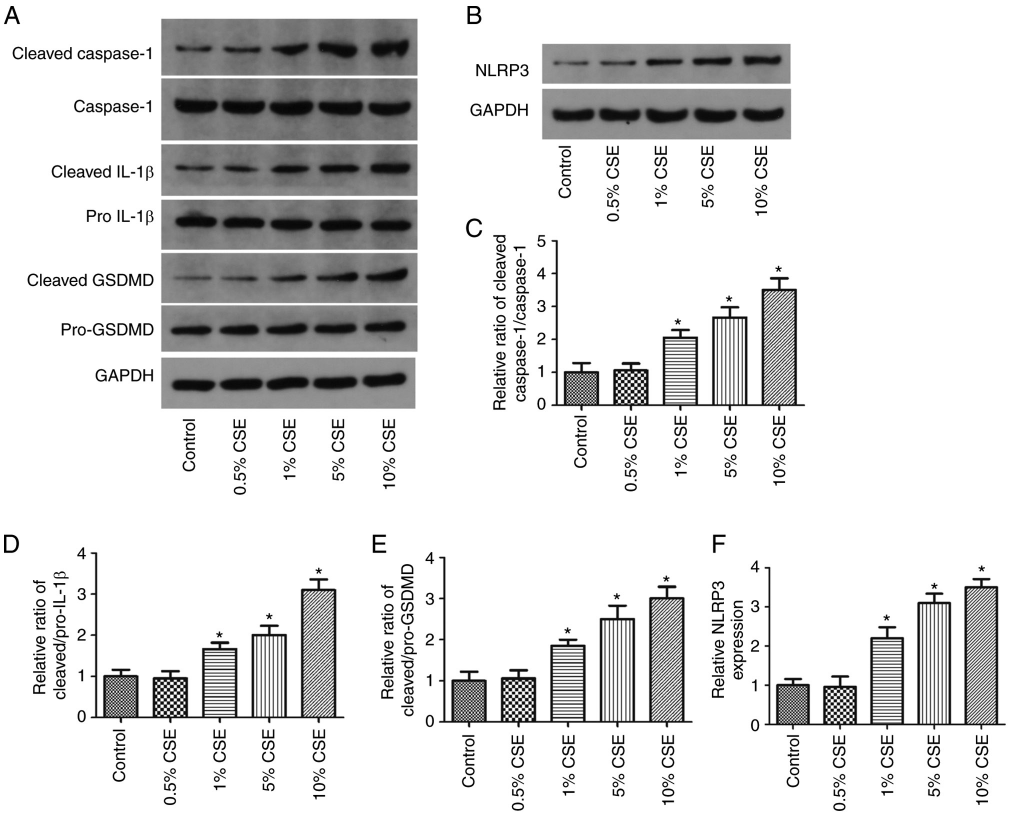

Figure 3. Effects of CSE on the expression of pyroptosis-related proteins in 16HBE cells. (A and B) Representative protein bands. (C-F) Results of quantitative analysis. Data are presented as the mean ± SD and are representative of three independent experiments. *P<0.05 compared with the control group. CSE, cigarette smoke extract; GSDMD, gasdermin D; NLRP3, NLR family pyrin domain containing 3.

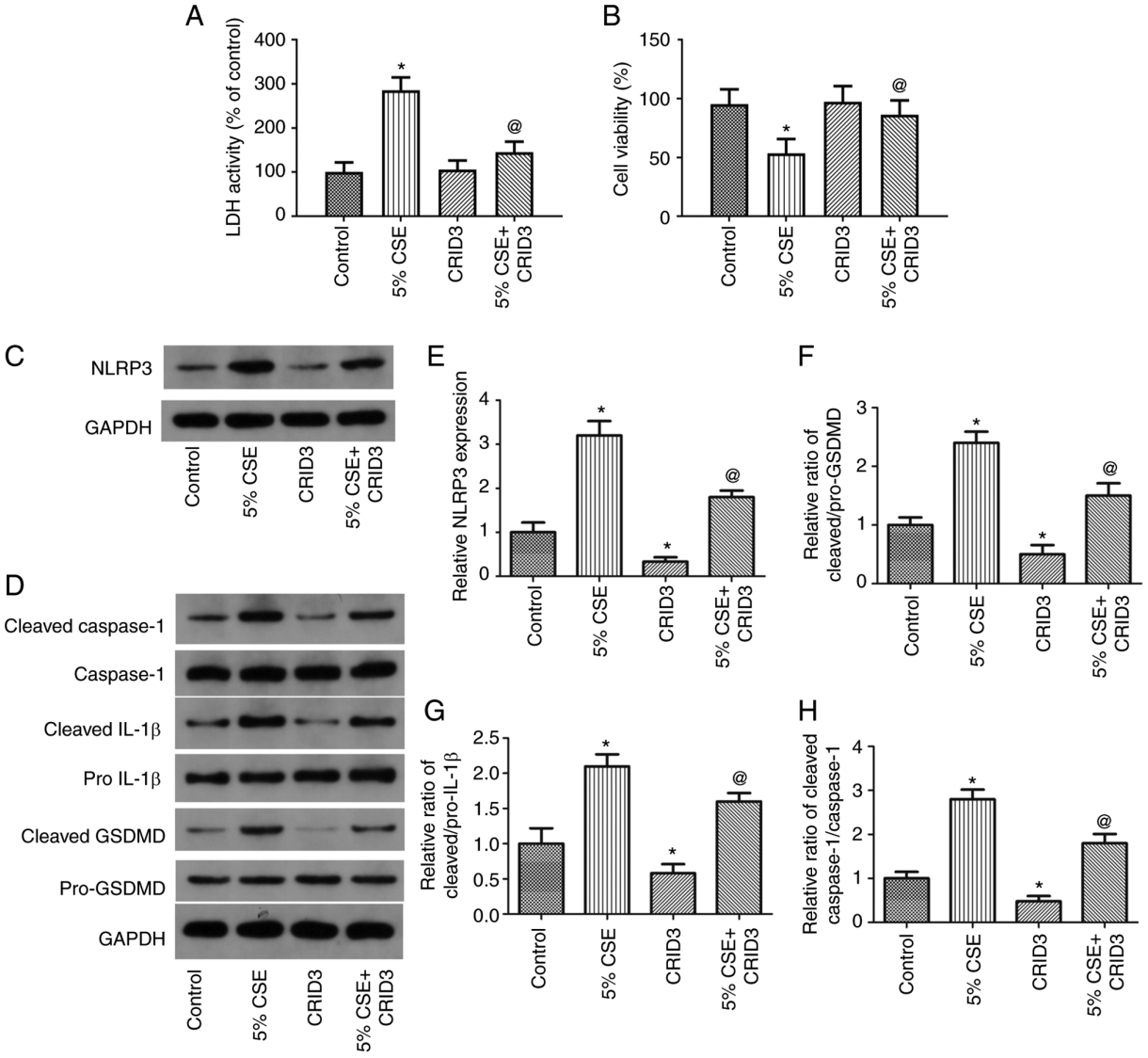

Figure 4. The NLRP3 inhibitor, CRID3, reverses the effects of CSE on the pyroptosis of 16HBE cells. To examine the role of NLRP3 in the CSE-induced pyroptosis of 16HBE cells, the cells were exposed to 5% CSE and treated with the NLRP3 inhibitor, CRID3, for 24 h. (A and B) LDH activity and cell viability, (C-H) as well as the expression levels of pyroptosis-related proteins were examined. Data are presented as the mean ± SD and are representative of three independent experiments. *P<0.05 compared with the control group; @P<0.05 compared with the CSE group. NLRP3, NLR family pyrin domain containing 3; GSDMD, gasdermin D; CRID3, cytokine release inhibitory drug 3; CSE, cigarette smoke extract; LDH, lactate dehydrogenase.

thus revealed that CSE promoted TLR4/NF-κB pathway activation in 16HBE cells, while this was inhibited by H_2S.

Effects of TLR4/NF-κB overexpression/knockdown on the CSE-induced pyroptosis of 16HBE cells. To examine the role of the TLR4/NF-κB pathway in the effects of NaHS on CSE-induced pyroptosis, the 16HBE cells were exposed to 5% CSE, and treated with NaHS and lentivirus overexpressing TLR4 or NF-κB. The transfection efficiency was determined using RT-qPCR (Fig. 7C and D). LDH activity, cell viability and the expression levels of pyroptosis-related proteins were then measured. As shown in Fig. 7A and B, transfection with TLR4 and NF-κB lentivirus significantly increased the LDH activity and decreased 16HBE cell viability compared with the 5% CSE + NaHS group. On the other hand, TLR4 and NF-κB lentivirus markedly increased the ratios of cleaved Caspase-1/Caspase-1 and cleaved GSDMD/pro-GSDMD (Fig. 7E-G). In addition, when TLR4 or NF-κB expression was silenced in the 16HBE cells by lentiviral transduction. The transfection efficiency was determined using RT-qPCR (Fig. 7J and K). It was found that TLR4 or NF-κB knockdown mimicked the effects of NaHS in terms of LDH activity, cell viability and the level of cleaved Caspase-1/Caspase-1 and cleaved GSDMD/pro-GSDMD (Fig. 7H, I and L-N). These findings revealed that the TLR4/NF-κB pathway was essential for the protective effect of H_2S against CSE-induced pyroptosis in 16HBE cells.

Discussion

Pyroptosis is a type of Caspase-1-dependent programmed cell death and is accompanied by an inflammatory reaction (4). When exogenous (bacteria and viruses) or endogenous (stress factors released when the cell is attacked) danger signals stimulate the cells, NF-κB activates NLRP3, which in turn activates Caspase-1 precursor, cleaves GSDMD protein and

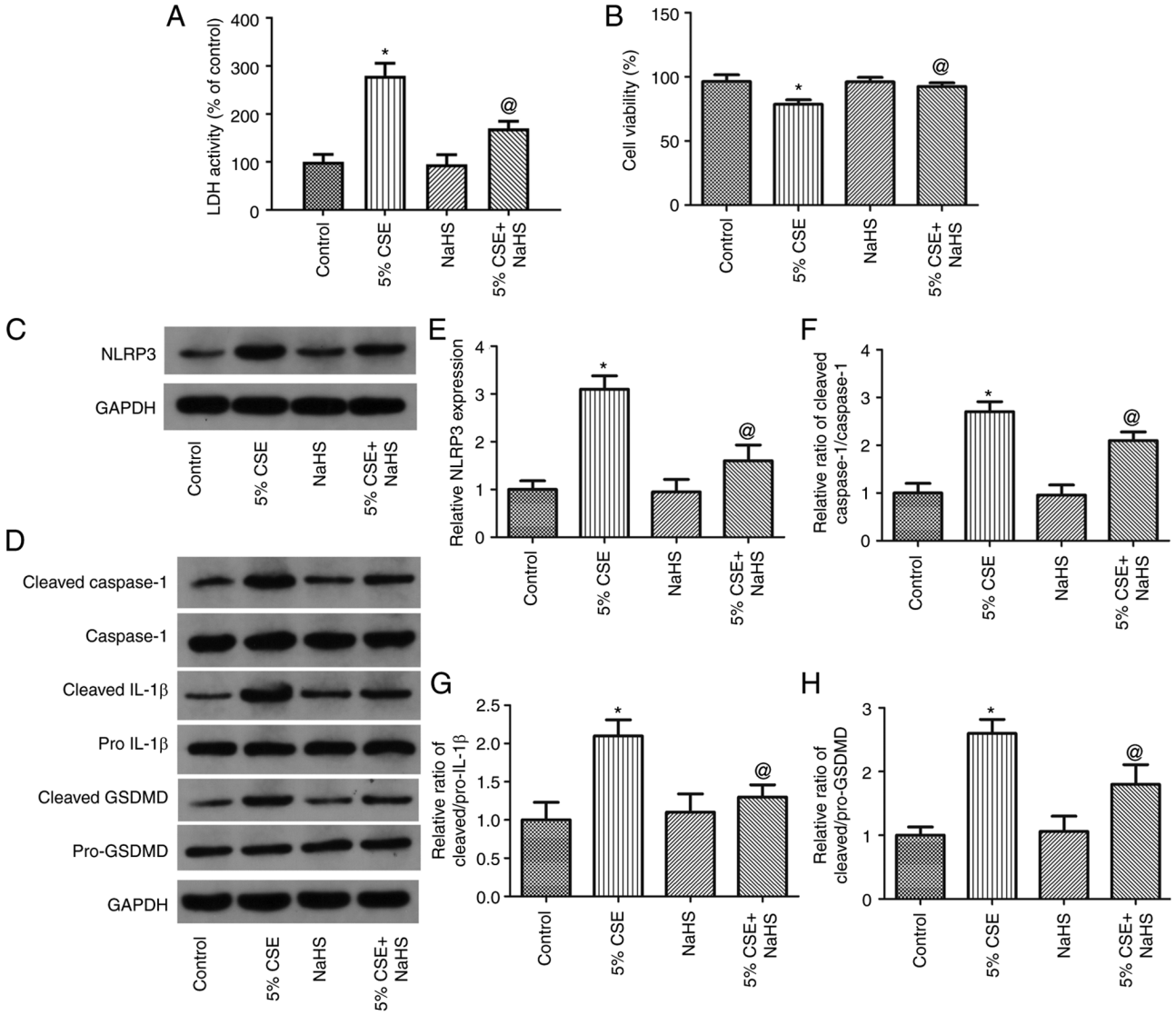

Figure 5. NaHS reverses the CSE-induced pyroptosis of 16HBE cells. To examine the effect of H2S on the CSE-induced pyroptosis of 16HBE cells, the cells were exposed to 5% CSE and treated with NaHS (an H2S donor) for 24 h. (A) LDH activity, (B) cell viability and (C-H) the expression levels of pyroptosis-related proteins were then measured. Data are presented as the mean ± SD and are representative of three independent experiments. $^{*}P<0.05$ compared with the control group; $^{@}P<0.05$ compared with the CSE group. CSE, cigarette smoke extract; H_2S, hydrogen sulfide; LDH, lactate dehydrogenase; GSDMD, gasdermin D; NaHS, sodium hydrosulfide.

releases N-terminal fragment. This recognizes and binds the phospholipids on the cell membrane and forms cell membrane pores, as well as loses the ability to control the entry and exit of substances, leading to cell osmotic pressure changes, cell lysis, the release of cell contents and cell death (5). NLRP3 is the basic component of the inflammasome in cell pyroptosis. Pyroptosis is closely associated with inflammatory lung diseases. As previously demonstrated in a mouse model of COPD, the activation of caspase-l, the production of IL-18 and IL-1B, and the inflow of neutrophils in bronchoalveolar lavage fluid of NLRP3-knockout mice were decreased, indicating the involvement of NLRP3 in COPD pathogenesis (30). The findings of the present study demonstrated that, in the CS-induced COPD model, cell pyroptosis was significantly activated. Compared with the control group, the expression level of GSDMD-N was increased in the CS group, as were NLRP3 expression and the ratios of cleaved Caspase-1/Caspase-1, cleaved IL-1β/pro-IL-1β and cleaved GSDMD/pro-GSDMD. The exposure of 16HBE cells to CSE induced an increase in the pyroptosis (as demonstrated by LDH leakage) and pyroptosis-related protein expression (NLRP3, cleaved Caspase-1, cleaved GSDMD and cleaved IL-1β) in a concentration-dependent manner. This finding is in accordance with earlier research (15,16). Previous animal studies have revealed that frequent exposure to CS can lead to an increase in the number of inflammatory factors in the alveolar space and lung parenchyma, leading to cell death (31,32). Thioredoxin interacting protein (TXNIP) combines with NLRP3 to form a complex in the process of COPD, which can initiate pyroptosis and promote inflammatory response through TXNIP overexpression, while the inhibition of TXNIP expression can reduce the formation of inflammatory bodies, improve cell viability and alleviate COPD progression (33,34).

GSDMD is the executor of cell pyroptosis. To demonstrate that GSDMD was cleaved by Caspase-11 at the preserved residual of d276, Kayagaki *et al* (35) used the CRISPR-Cas9

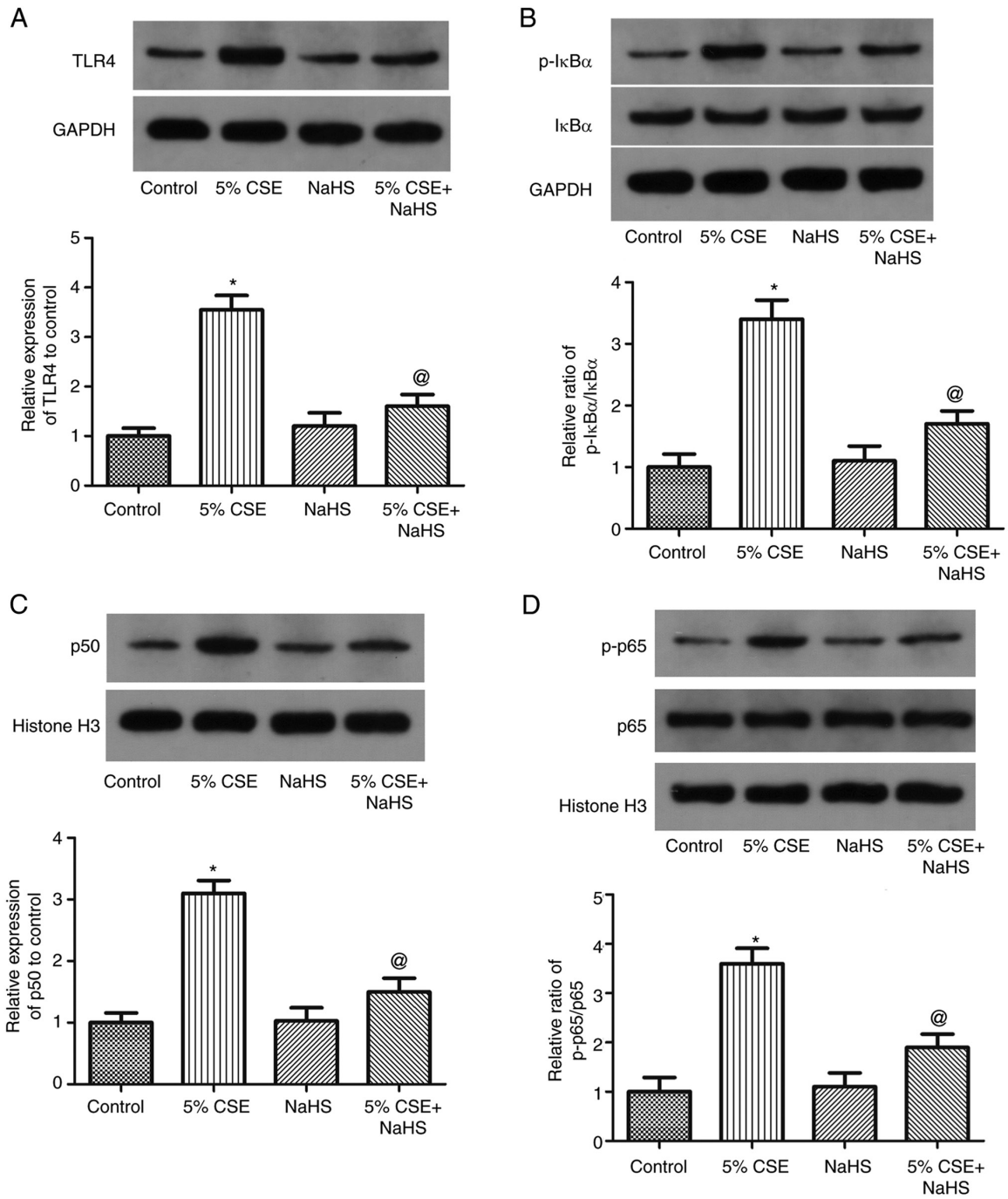

Figure 6. NaHS reduces CSE-induced TLR4/NF-κB pathway activation in 16HBE cells. (A-D) To analyze the role of the TLR4/NF-κB pathway in the effects of H_2S on the CSE-induced pyroptosis of 16HBE cells, the cells we exposed to 5% CSE and treated with NaHS (H_2S donor) for 24 h, and the expression levels of IκBα, p-IκBα, NF-κB p50, NF-κB p65 and NF-κB p-p65 were then measured in 16HBE cells. Data are presented as the mean ± SD. *P<0.05 compared with the control group; @P<0.05 compared with the CSE group. CSE, cigarette smoke extract; TLR4, Toll-like receptor 4; NaHS, sodium hydrosulfide.

genome editing technique to produce the GSDMD-C- and GSDMD-N-terminal domains, which eventually led to cell pyroptosis. GSDMD is an essential pyroptosis substance for all inflammatory caspases, and is a common substrate. The results of the present study demonstrated that the GSDMD inhibitor, NSA, reversed the increased pyroptosis (as demonstrated by LDH leakage) and enhanced cell viability, indicating that pyroptosis played an essential role in the cytotoxic effects of CSE on 16HBE cells. This result also suggested that the CSE-induced pyroptosis of 16HBE cells was GSDMD-dependent.

NLRP3, as an important inflammatory body, can be activated via two mechansims. On the one hand, it can stimulate TLR4 and NF-κB and can modulate the expression levels of adhesion and inflammatory factors, thus producing pro-IL-18 and pro-IL-1β (36). On the other hand, NLRP3 binds with apoptosis-associated speck-like protein containing a caspase activation and recruitment domain to form an activated NLRP3 inflammasome, which then cleaves Caspase-1 to promote the formation and maturation of pro-IL-18 and pro-IL-1β, thus mediating pyroptosis (37). The cell experimental results of the present study demonstrated that the

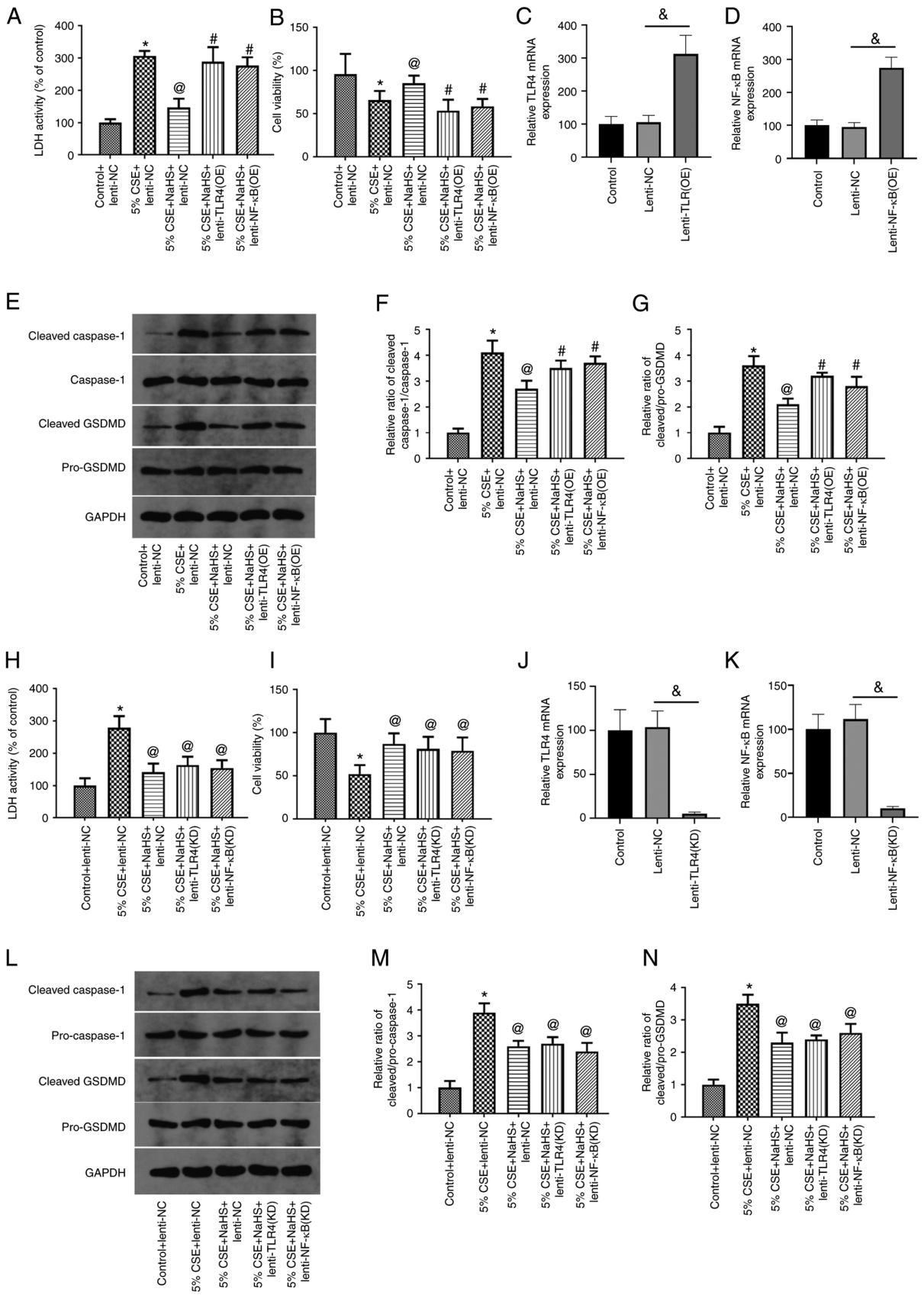

Figure 7. Overexpression of TLR4/NF-κB abolishes the suppressive effects of NaHS on the CSE-induced pyroptosis of 16HBE cells. (A-G) 16HBE cells were exposed to 5% CSE, and treated with NaHS and lentivirus overexpressing TLR4 or NF-κB. (A) LDH activity, (B) cell viability and (E-G) the expression levels of pyroptosis-related proteins were then measured. (C and D) The transfection efficiency was measured using RT-qPCR. (H-N) 16HBE cells were exposed to 5% CSE, and then treated with NaHS and transfected with lentivirus to knockdown TLR4 or NF-κB. (H) LDH activity, (I) cell viability and (L-N) the expression levels of pyroptosis-related proteins were then measured. (J and K) The transfection efficiency was measured using RT-qPCR. Data are presented as the mean ± SD and are representative of three independent experiments. $^{\#}$P<0.05 compared with the 5% CSE + NaHS + Lenti-NC group; *P<0.05 compared with the control + Lenti-NC group; $^{@}$P<0.05 compared with the 5% CSE + Lenti-NC group; $^{\&}$P<0.05 between lenti-NC and transfection groups. TLR4, Toll-like receptor 4; CSE, cigarette smoke extract; LDH, lactate dehydrogenase; GSDMD, gasdermin D; NaHS, sodium hydrosulfide; RT-qPCR, reverse transcription-quantitative PCR.

NLRP3 inhibitor, CRID3, significantly reduced pyroptosis (as demonstrated by LDH leakage) and reduced the expression of pyroptosis-related protein (NLRP3, cleaved IL-1β, Caspase-1 and GSDMD) in 16HBE cells, indicating that the CSE-induced pyroptosis of 16HBE cells was NLRP3-dependent. In combination, these results support the conclusion that CS induces the pyroptosis of human bronchial epithelial cells in a NLRP3/GSDMD-dependent manner.

Several studies have reported that H_2S plays a protective role against cell injury by deterring NLRP3 inflammasome activation. In human acute monocytic leukemia cells, H_2S has been shown to inhibit NLRP3 protein expression, as well as the LPS-induced Caspase-1 expression (38). It has also been demonstrated that H_2S attenuates LPS-induced acute kidney damage in mice by preventing the formation of the NLRP3 inflammasome (39). Furthermore, H_2S reduces ischemia-reperfusion injury by impeding the inflammatory response, as well as TLR-mediated oxidative stress (40,41). H_2S has also been found to inhibit the inflammatory response by inhibiting NF-κB activity, as well as by reducing the expression level of TNF-α (42). The effects of inhaled H_2S on lung injury were investigated in the present study, and its impact on CS-induced pyroptosis in rats was then investigated. The results demonstrated that inflammatory cell infiltration and alveolar septum thickening were markedly alleviated by H_2S, and it also decreased GSDMD-N expression in the lungs. Furthermore, the expression levels of pyroptosis-related proteins (NLRP3, cleaved IL-1β, cleaved Caspase-1 and cleaved GSDMD) were markedly decreased by H_2S, indicating that inhaled H_2S inhibited pyroptosis in the model of CS-induced COPD. To further examine the mechanisms of H_2S on the CS-induced pyroptosis of lung cells, the 16HBE cells were exposed to CSE and treated with NaHS (H_2S donor), and the pyroptosis (as demonstrated by LDH leakage), viability and the expression levels of pyroptosis-related proteins were then measured. Similar to the results of the *in vivo* experiments, H_2S significantly attenuated the effects of CSE on pyroptosis, cell viability and pyroptosis-related protein expression. It was thus indicated that H_2S inhibited pyroptosis by decreasing NLRP3 expression and GSDMD activation.

The contribution of the TLR4/NF-κB signaling pathway to the inflammatory response and other pathological changes has been demonstrated (43). TLRs, which can activate the innate immune system, are a family of pattern recognition receptors. The primary function of TLR4 is to recognize exogenous molecules from pathogens (such as LPS). TLR4 can be recognized by the metabolites of bacteria, viruses and other pathogens (44). At the same time, TLR4, as a specific recognition receptor of LPS, can be activated in numerous immune cells, such as macrophages and B-lymphocytes (36). Previous studies have revealed that TLR4 is highly expressed in BV-2 cells, RAW264.7 macrophages and C57BL/6 mice exposed to LPS (45-47). In the present study, to evaluate the role of TLR4 in the effects of H_2S on the CSE-induced pyroptosis of 16HBE cells, the cells were treated with 5% CSE and NaHS (H_2S donor) for 24 h. TLR4 expression in the 16HBE cells was then assessed. TLR4 expression in the 16HBE cells was increased by CSE, but was partly reversed by NaHS. These findings suggested that in 16HBE cells, CSE activated TLR4, while this was inhibited by H_2S.

NF-κB is an ubiquitous transcription factor mediating the cytoplasmic-nuclear signaling pathway. NF-κB exists in the form of a dimer and its role in the development of different inflammation-related illnesses has been proven, such as via its involvement in cell apoptosis and proliferation (48). Liu *et al* (49) revealed that melatonin alleviated inflammatory pyroptosis in mouse adipose tissue by modulating the NF-κB/GSDMD signaling pathway, while Chen *et al* (50) reported that never in mitosis gene A (NIMA)-related kinase 7 (NEK7) interacted with NLRP3 to regulate pyroptosis through NF-κB signaling in inflammatory bowel disease. The study by Shao *et al* (51) demonstrated that traumatic brain injury-induced acute lung injury was alleviated by ghrelin through the pyroptosis/NF-κB pathway, while Tian *et al* (52) found that exposure to ozone stimulated pyroptosis in the lungs of rats through the TLR2/4/NF-κB/NLRP3 signaling pathway. Therefore, it was hypothesized that NF-κB may be the key effector molecule of CSE-induced cell pyroptosis.

In the present study, to examine the function of the NF-κB pathway, the cells were exposed to 5% CSE and treated with NaHS, and the expression levels of IκBα, p-IκBα, NF-κB p50, NF-κB p65 and NF-κB p-p65 were measured in the 16HBE cells. The ratios of NF-κB p-p65/p65 and p-IκBα/IκBα, as well as the expression levels of NF-κB p50 in 16HBE cells were increased by CSE, which these were all partly reversed by NaHS. These findings suggested that CSE induced the activation of the TLR4/NF-κB pathway in 16HBE cells, while this was inhibited by H_2S. A recent study reported that NF-κB was the prominent GSDMD transcription factor (49). Under normal conditions, the C-terminal of GSDMD automatically inhibits the pore-forming activity of the N-terminal (53). When NF-κB is activated, it activates the inflammasomes and Caspase-1, and causes the separation of the N- and C-terminals of GSDMD. Under external stimulation, activated TLR4 activates the IκB kinase (IKK) complex through the myeloid differentiation primary response 88-dependent pathway, leading to IKK phosphorylation. Subsequently, IKK is degraded through the ubiquitin-proteasome pathway, thus releasing NF-κB and promoting its entry into the nucleus from the cytoplasm, thereby inducing the expression levels of inflammation-related genes (54-56). In the present study, to analyze the role of the TLR4/NF-κB pathway, 16HBE cells were exposed to CSE, and treated with NaHS and lentivirus overexpressing TLR4 or NF-κB; LDH activity, cell viability and pyroptosis were then measured. NF-κB and TLR4 overexpression markedly increased pyroptosis (as demonstrated by LDH leakage) and decreased the viability of 16HBE cells. Furthermore, the ratios of cleaved GSDMD/pro-GSDMD and cleaved Caspase-1/Caspase-1 were markedly increased, indicating that the effect of H_2S on cell pyroptosis was diminished by TLR4 and NF-κB overexpression. As TLR4 or NF-κB overexpression abrogated the therapeutic effects of NaHS, it was suggested that NaHS reduced pyroptosis by inhibiting TLR4/NF-κB signaling. Moreover, in order to further strengthen the results, the expression of TLR4 and NF-κB was silenced in 16HBE cells, followed by exposure to CSE and treatment with NaHS. It was found that TLR4 or NF-κB knockdown mimicked the effects of NaHS in terms of cell viability and the level of cleaved Caspase-1/Caspase-1 and cleaved GSDMD/pro-GSDMD. In combination, these results

indicated that the TLR4/NF-κB pathway may be essential for the protective effects of H_2S against the CSE-induced pyroptosis of 16HBE cells.

In conclusion, the present study demonstrated that H_2S alleviated lung injury and pyroptosis in a model of CS-induced COPD by inhibiting the activation of the TLR4/NF-κB signaling pathway. These findings suggest the importance of pyroptosis in the development of COPD and provide an experimental framework in which H_2S and drugs targeting the TLR4/NF-κB pathway may be utilized for protection against COPD.

Acknowledgements

Not applicable.

Funding

No funding was received.

Availability of data and materials

The datasets used or analyzed during the current study are available from the corresponding author on reasonable request.

Authors' contributions

CY and YL contributed to the conception of the study. LW and JM performed all of the experiments. LW and JM contributed significantly to the analysis of the results of the experiments and to manuscript preparation. CW performed the data analyses and wrote the manuscript. YW helped perform the analysis of the proofs manuscript and provided constructive discussions. LW, CW and JM confirm the authenticity of all the raw data. All authors have read and approved the final manuscript.

Ethics approval and consent to participate

The animal procedures were approved by the Animal Ethics Committee of the Hebei Chest Hospital Animal Center and complied with the Guide of the Care and Use of Laboratory Animals published by NIH (NIH Pub. no. 85-23, revised 1996).

Patient consent for publication

Not applicable.

Competing interests

The authors declare that they have no competing interests.

References

1. Zhou M, Wang H, Zhu J, Chen W, Wang L, Liu S, Li Y, Wang L, Liu Y, Yin P, *et al*: Cause-specific mortality for 240 causes in China during 1990-2013: A systematic subnational analysis for the global burden of disease study 2013. Lancet 387: 251-272, 2016.
2. López-Campos JL, Tan W and Soriano JB: Global burden of COPD. Respirology 21: 14-23, 2016.
3. Saetta M, Turato G, Maestrelli P, Mapp CE and Fabbri LM: Cellular and structural bases of chronic obstructive pulmonary disease. Am J Respir Crit Care Med 163: 1304-1309, 2001.
4. Churg A, Wang RD, Tai H, Wang X, Xie C, Dai J, Shapiro SD and Wright JL: Macrophage metalloelastase mediates acute cigarette smoke-induced inflammation via tumor necrosis factor-alpha release. Am J Respir Crit Care Med 167: 1083-1089, 2003.
5. Wang C, Xu J, Yang L, Xu Y, Zhang X, Bai C, Kang J, Ran P, Shen H, Wen F, *et al*: Prevalence and risk factors of chronic obstructive pulmonary disease in China (the China Pulmonary Health [CPH] study): A national cross-sectional study. Lancet 391: 1706-1717, 2018.
6. US Preventive Services Task Force (USPSTF), Siu AL, Bibbins-Domingo K, Grossman DC, Davidson KW, Epling JW Jr, García FA, Gillman M, Kemper AR, Krist AH, *et al*: Screening for chronic obstructive pulmonary disease: US preventive services task force recommendation statement. JAMA 315: 1372-1377, 2016.
7. Shi J, Gao W and Shao F: Pyroptosis: Gasdermin-mediated programmed necrotic cell death. Trends Biochem Sci 42: 245-254, 2017.
8. Vande Walle L and Lamkanfi M: Pyroptosis. Curr Biol 26: R568-R572, 2016.
9. Dong ZW and Yuan YF: Juglanin suppresses fibrosis and inflammation response caused by LPS in acute lung injury. Int J Mol Med 41: 3353-3365, 2018.
10. Li Y, Song D, Bo F, Deng M and Tang X: Diazepam inhibited lipopolysaccharide (LPS)-induced pyroptotic cell death and alleviated pulmonary fibrosis in mice by specifically activating $GABA_A$ receptor α4-subunit. Biomed Pharmacother 118: 109239, 2019.
11. Pinkerton JW, Kim RY, Robertson AAB, Hirota JA, Wood LG, Knight DA, Cooper MA, O'Neill LAJ, Horvat JC and Hansbro PM: Inflammasomes in the lung. Mol Immunol 86: 44-55, 2017.
12. Wang YC, Liu QX, Zheng Q, Liu T, Xu XE, Liu XH, Gao W, Bai XJ and Li ZF: Dihydromyricetin alleviates sepsis-induced acute lung injury through inhibiting NLRP3 inflammasome-dependent pyroptosis in mice model. Inflammation 42: 1301-1310, 2019.
13. Xu WJ, Wang XX, Jin JJ, Zou Q, Wu L, Lv TF, Wan B, Zhan P, Zhu SH, Liu HB, *et al*: Inhibition of GGPPS1 attenuated LPS-induced acute lung injury and was associated with NLRP3 inflammasome suppression. Am J Physiol Lung Cell Mol Physiol 316: L567-L577, 2019.
14. Tsai YM, Chiang KH, Hung JY, Chang WA, Lin HP, Shieh JM, Chong IW and Hsu YL: Der f1 induces pyroptosis in human bronchial epithelia via the NLRP3 inflammasome. Int J Mol Med 41: 757-764, 2018.
15. Zhang MY, Jiang YX, Yang YC, Liu JY, Huo C, Ji XL and Qu YQ: Cigarette smoke extract induces pyroptosis in human bronchial epithelial cells through the ROS/NLRP3/caspase-1 pathway. Life Sci 269: 119090, 2021.
16. Zhu Z, Lian X, Su X, Wu W, Zeng Y and Chen X: Exosomes derived from adipose-derived stem cells alleviate cigarette smoke-induced lung inflammation and injury by inhibiting alveolar macrophages pyroptosis. Respir Res 23: 5, 2022.
17. Wang R: Hydrogen sulfide: The third gasotransmitter in biology and medicine. Antioxid Redox Signal 12: 1061-1064, 2010.
18. Oláh G, Módis K, Törö G, Hellmich MR, Szczesny B and Szabo C: Role of endogenous and exogenous nitric oxide, carbon monoxide and hydrogen sulfide in HCT116 colon cancer cell proliferation. Biochem Pharmacol 149: 186-204, 2018.
19. Xu X, Li H, Gong Y, Zheng H and Zhao D: Hydrogen sulfide ameliorated lipopolysaccharide-induced acute lung injury by inhibiting autophagy through PI3K/Akt/mTOR pathway in mice. Biochem Biophys Res Commun 507: 514-518, 2018.
20. Liu M, Li Z, Liang B, Li L, Liu S, Tan W, Long J, Tang F, Chu C and Yang J: Hydrogen sulfide ameliorates rat myocardial fibrosis induced by thyroxine through PI3K/AKT signaling pathway. Endocr J 65: 769-781, 2018.
21. George AK, Singh M, Homme RP, Majumder A, Sandhu HS and Tyagi SC: A hypothesis for treating inflammation and oxidative stress with hydrogen sulfide during age-related macular degeneration. Int J Ophthalmol 11: 881-887, 2018.
22. Wang L, Meng J, Wang C, Yang C, Wang Y, Li Y and Li Y: Hydrogen sulfide alleviates cigarette smoke-induced COPD through inhibition of the TGF-β1/smad pathway. Exp Biol Med (Maywood) 245: 190-200, 2020.
23. National Research Council (US) Institute for Laboratory Animal Research: Guide for the Care and Use of Laboratory Animals. National Academies Press, Washington, DC, 1996.
24. Ke Q, Yang L, Cui Q, Diao W, Zhang Y, Xu M and He B: Ciprofibrate attenuates airway remodeling in cigarette smoke-exposed rats. Respir Physiol Neurobiol 271: 103290, 2020.

25. Hosseini A, Rasaie D, Soleymani Asl S, Nili Ahmadabadi A and Ranjbar A: Evaluation of the protective effects of curcumin and nanocurcumin against lung injury induced by sub-acute exposure to paraquat in rats. Toxin Rev 40: 1233-1241, 2019.
26. Song B, Ye L, Wu S and Jing Z: Long non-coding RNA MEG3 regulates CSE-induced apoptosis and inflammation via regulating miR-218 in 16HBE cells. Biochem Biophys Res Commun 521: 368-374, 2020.
27. Ding Y, Liu P, Chen ZL, Zhang SJ, Wang YQ, Cai X, Luo L, Zhou X and Zhao L: Emodin attenuates lipopolysaccharide-induced acute liver injury via inhibiting the TLR4 signaling pathway in vitro and in vivo. Front Pharmacol 9: 962, 2018.
28. Livak KJ and Schmittgen TD: Analysis of relative gene expression data using real-time quantitative PCR and the 2(-Delta Delta C(T)) method. Methods 25: 402-408, 2001.
29. Zhang Y, Xia G, Zhang Y, Liu J, Liu X, Li W, Lv Y, Wei S, Liu J and Quan J: Palmitate induces VSMC apoptosis via toll like receptor (TLR)4/ROS/p53 pathway. Atherosclerosis 263: 74-81, 2017.
30. Yang W, Ni H, Wang H and Gu H: NLRP3 inflammasome is essential for the development of chronic obstructive pulmonary disease. Int J Clin Exp Pathol 8: 13209-13216, 2015.
31. Lee S, Suh GY, Ryter SW and Choi AM: Regulation and function of the nucleotide binding domain leucine-rich repeat-containing receptor, pyrin domain-containing-3 inflammasome in lung disease. Am J Respir Cell Mol Biol 54: 151-160, 2016.
32. Eltom S, Belvisi MG, Stevenson CS, Maher SA, Dubuis E, Fitzgerald KA and Birrell MA: Role of the inflammasome-caspase1/11-IL-1/18 axis in cigarette smoke driven airway inflammation: An insight into the pathogenesis of COPD. PLoS One 9: e112829, 2014.
33. Barnes PJ: Inflammatory mechanisms in patients with chronic obstructive pulmonary disease. J Allergy Clin Immunol 138: 16-27, 2016.
34. Heo MJ, Kim TH, You JS, Blaya D, Sancho-Bru P and Kim SG: Alcohol dysregulates miR-148a in hepatocytes through FoxO1, facilitating pyroptosis via TXNIP overexpression. Gut 68: 708-720, 2019.
35. Kayagaki N, Stowe IB, Lee BL, O'Rourke K, Anderson K, Warming S, Cuellar T, Haley B, Roose-Girma M, Phung QT, *et al*: Caspase-11 cleaves gasdermin D for non-canonical inflammasome signalling. Nature 526: 666-671, 2015.
36. Ding J, Wang K, Liu W, She Y, Sun Q, Shi J, Sun H, Wang DC and Shao F: Pore-forming activity and structural autoinhibition of the gasdermin family. Nature 535: 111-116, 2016.
37. Liang H and Liu Y: Gasdermins pore cell membrane to pyroptosis. Sci China Life Sci 59: 1090-1092, 2016.
38. Yue LM, Gao YM and Han BH: Evaluation on the effect of hydrogen sulfide on the NLRP3 signaling pathway and its involvement in the pathogenesis of atherosclerosis. J Cell Biochem 120: 481-492, 2019.
39. Chen Y, Jin S, Teng X, Hu Z, Zhang Z, Qiu X, Tian D and Wu Y: Hydrogen sulfide attenuates LPS-induced acute kidney injury by inhibiting inflammation and oxidative stress. Oxid Med Cell Longev 2018: 6717212, 2018.
40. Tan Z, Shi Y, Yan Y, Liu W, Li G and Li R: Impact of endogenous hydrogen sulfide on toll-like receptor pathway in renal ischemia/reperfusion injury in rats. Ren Fail 37: 727-733, 2015.
41. Han SJ, Kim JI, Park JW and Park KM: Hydrogen sulfide accelerates the recovery of kidney tubules after renal ischemia/reperfusion injury. Nephrol Dial Transplant 30: 1497-1506, 2015.
42. Chen X, Xu W, Wang Y, Luo H, Quan S, Zhou J, Yang N, Zhang T, Wu L, Liu J, *et al*: Hydrogen sulfide reduces kidney injury due to urinary-derived sepsis by inhibiting NF-κB expression, decreasing TNF-α levels and increasing IL-10 levels. Exp Ther Med 8: 464-470, 2014.
43. Fu Y, Liu B, Zhang N, Liu Z, Liang D, Li F, Cao Y, Feng X, Zhang X and Yang Z: Magnolol inhibits lipopolysaccharide-induced inflammatory response by interfering with TLR4 mediated NF-κB and MAPKs signaling pathways. J Ethnopharmacol 145: 193-199, 2013.
44. Varshney D, Singh S, Sinha E, Mohanty KK, Kumar S, Kumar Barik S, Patil SA and Katara P: Systematic review and meta-analysis of human Toll-like receptors genetic polymorphisms for susceptibility to tuberculosis infection. Cytokine 152: 155791, 2022.
45. Zhou P, Weng R, Chen Z, Wang R, Zou J, Liu X, Liao J, Wang Y, Xia Y and Wang Q: TLR4 signaling in MPP+-induced activation of BV-2 cells. Neural Plast 2016: 5076740, 2016.
46. Huang H, Park PH, McMullen MR and Nagy LE: Mechanisms for the anti-inflammatory effects of adiponectin in macrophages. J Gastroenterol Hepatol 23 (Suppl 1): S50-S53, 2008.
47. Säfholm J, Lövdahl C, Swedin L, Boels PJ, Dahlén SE, Arner A and Adner M: Inflammation-induced airway smooth muscle responsiveness is strain dependent in mice. Pulm Pharmacol Ther 24: 361-366, 2011.
48. Soleimani A, Rahmani F, Ferns GA, Ryzhikov M, Avan A and Hassanian SM: Role of the NF-κB signaling pathway in the pathogenesis of colorectal cancer. Gene 726: 144132, 2020.
49. Liu Z, Gan L, Xu Y, Luo D, Ren Q, Wu S and Sun C: Melatonin alleviates inflammasome-induced pyroptosis through inhibiting NF-κB/GSDMD signal in mice adipose tissue. J Pineal Res 63, 2017.
50. Chen X, Liu G, Yuan Y, Wu G, Wang S and Yuan L: NEK7 interacts with NLRP3 to modulate the pyroptosis in inflammatory bowel disease via NF-κB signaling. Cell Death Dis 10: 906, 2019.
51. Shao XF, Li B, Shen J, Wang QF, Chen SS, Jiang XC and Qiang D: Ghrelin alleviates traumatic brain injury-induced acute lung injury through pyroptosis/NF-κB pathway. Int Immunopharmacol 79: 106175, 2020.
52. Tian L, Yan J, Li K, Zhang W, Lin B, Lai W, Bian L, Liu H, Xi Z and Liu X: Ozone exposure promotes pyroptosis in rat lungs via the TLR2/4-NF-κB-NLRP3 signaling pathway. Toxicology 450: 152668, 2021.
53. Liu Z, Wang C, Rathkey JK, Yang J, Dubyak GR, Abbott DW and Xiao TS: Structures of the gasdermin D C-terminal domains reveal mechanisms of autoinhibition. Structure 26: 778-784.e3, 2018.
54. Ayala-Cuellar AP, Cho J and Choi KC: Toll-like receptors: A pathway alluding to cancer control. J Cell Physiol 234: 21707-21715, 2019.
55. Lei J, Fu Y, Zhuang Y, Zhang K and Lu D: miR-382-3p suppressed IL-1β induced inflammatory response of chondrocytes via the TLR4/MyD88/NF-κB signaling pathway by directly targeting CX43. J Cell Physiol 234: 23160-23168, 2019.
56. Chen Z, Liu Q, Zhu Z, Xiang F, Wu R and Kang X: Toll-like receptor 4 contributes to uterine activation by upregulating pro-inflammatory cytokine and CAP expression via the NF-κB/P38MAPK signaling pathway during pregnancy. J Cell Physiol 235: 513-525, 2020.